SHIMADZU
Excellence in Science

Application Note

No. 97

Life Science

Pharmacokinetic Analysis Using iMScope™ QT During Corn and Soybean Seed Treatment with Pesticides

Shuichi Shimma[1,2,3], Yumi Saito[1], Takushi Yamamoto[4], Kaoru Nakagawa[4], Yumi Unno[4], Takuya Inoue[5]、Fukumatsu Iwahashi[5]

Life Science

Images were generated using Adobe Firefly.

■ Abstract

Pesticide seed treatments effectively protect crops early in the seeding process, allowing for less use of fungicide later. Consequently, it is implemented in significant agricultural products such as corn, soybeans, wheat, and cotton. Different distributions of pesticides on treated seeds can be visualized depending on the seeds' structures and physical properties, which have been not well studied. In this application note, mass spectrometry imaging using iMScope QT was performed to visualize the distribution of a fungicide (ethaboxam) within coated corn and soybean seeds. Contrasting distribution patterns were observed in corn and soybean at the pre-sowing stage, which were thought to depend on those seed structures. Information on the distribution of ethaboxam after sowing is also expected to provide data that will contribute to a better understanding of fungicide delivery pathways in plants. This new analytical method will enable us to obtain time-dependent and dynamic information on fungicides that have not been available before and will be a useful tool that can be widely applied in the development and use of pesticides in the future [1].

1 Department of Biotechnology, Graduate School of Engineering, Osaka University
2 The University of Osaka and Shimadzu Analyticai Innovation Research Laboratories
3 Institute for Open and Transdisciplinary Research Initiatives
4 Solutions COE, Analytical & Measuring Instruments Division, SHIMADZU CORPRATION
5 Health & Crop Sciences Research Laboratory, SUMITOMO CHEMICAL

1. Introduction

Matrix-assisted laser desorption/ionization mass spectrometry imaging (MALDI-MSI) is used in various fields as a Label-free imaging method. Until now, most of the studies using MALDI-MSI have been conducted in the fields of medicine and pharmacology [2, 3]. Recently, however, MALDI-MSI has also been applied to research fields in plants, such as visualization of secondary metabolite distribution[4-8] and evaluation of pesticide kinetics[9]. The usefulness of this technique has attracted much interest in the visualization of pesticide distribution, which has so far relied on the limited method of autoradiography with the use of 14C-labeled pesticides, and in the time-dependent dynamic movement of pesticides within plants, for which there is currently only limited information[10, 11]. Since the introduction of penetrating fungicides for seed treatments in the United States in the 1970s, seed treatments such as seed coatings, film coatings, and pellet treatments have provided efficient crop protection in the early seeding period and have enabled the reduction of pesticide application to crops. This seed treatment technology has been commercialized for major crops such as corn, soybean, wheat, and cotton[12-14]. Many pesticide seed treatment methods have been studied and optimized for each crop. It is believed that pesticides coated on seeds are either transferred directly into the plant body, transiently into the soil, or finally into target plant tissues by reabsorption after transfer into the soil[15]. Currently, however, there is limited information on the mechanisms by which chemical ingredients used in seed treatments are translocated within plant tissues.

This information on the transfer mechanisms of medicinal components could contribute to a better understanding of their actual effects on plants. In this study, we attempted to use MALDI-MSI to gain insight into the distribution of active ingredients used in seed treatments. For this purpose, we coated dried corn and soybean seeds with the fungicide ethaboxam[16-18] and visualized their distribution in the seeds before and after sowing. Note that ethaboxam is a pesticide that is particularly effective against egg fungus and is used for spraying and seed treatment. In this experiment, seeds were sectioned and transferred using cryotape for MALDI-MSI.
. Using these methods, we have demonstrated that MALDI-MSI is a useful tool for evaluating the distribution of chemical components in seeds after seed treatment.

2. Method

2-1. Reagents
α-cyano-4-hydroxycinnamic acid (α-CHCA) was purchased from Merck (Maryland, USA). Methanol, acetonitrile, formic acid, 2-propanol, and ultrapure water were purchased from Fujifilm Wako Pure Chemical Industries (Osaka, Japan). All reagents were of LC-MS grade.

2-2. Treatment of soybean and corn seeds with ethaboxam. Test solutions for seed treatment were prepared by diluting ethaboxam 34.2% (w/v) solution (INTEGO solo fungicide, Nufarm, Calgary, Canada) with water. Soybean (variety: Hatayutaka) seeds were treated at a dose of 75.0 g a.i. (a.i.: active ingredient)/100 kg seed as a final concentration of ethaboxam. On the other hand, corn (variety P1547) seeds were treated with a final concentration of ethaboxam at a dose of 37.5 g a.i. / 100 kg seed. For the seed treatments, 50 g each of soybean and corn seeds were mixed in 0.5 L plastic bags containing 260 µL and 490 µL of the test solution, respectively, to coat the seeds. Seeds treated with an empty formulation were also prepared as a negative control.

2-3. Seed germination.
Plastic cups (0.75 oz capacity) with holes in the bottom were filled to about 80% soil content and coated soybean or corn seeds were sown to a depth of about 1 cm below the soil surface. After sowing, the cups were placed in trays filled with water to a depth of about 2 cm and allowed to grow for 5 days in a room at 25 ºC .

2-4. Preparation of seed sections.
Pre- and post-seeding seeds were flash-frozen in liquid nitrogen and then sectioned at -20 ºC using a cryostat (CM1950; Leica, Nussloch, Germany). Frozen sections were prepared by embedding in 4% carboxymethylcellulose (SECTION-LAB, Yokohama, Japan). Cryofilm (SECTION-LAB, Yokohama, Japan) was used for sectioning. All frozen tissue was sectioned at 15 µm thickness, and the Cryofilm from which the sections were collected was attached to indium tin oxide (ITO)-coated glass slides (100 Ω/m2 without anti-peel coating; Matsunami Glass, Osaka, Japan) using conductive double-sided tape (conductive nonwoven tape; 3M Corporation, Minnesota, USA).

2-5. Matrix application.
Matrix deposition equipment (Figure 1A, iMLayer™; Shimadzu Corporation, Kyoto, Japan) was used to deposit α-CHCA at 250 ºC to a thickness of 0.7 µm on ITO glass loaded with seed sections.

2-6. MALDI-MSI Analysis.
MALDI-MSI analysis was performed using an atmospheric pressure matrix-assisted laser desorption/ionization quadrupole time-of-flight mass spectrometer iMScope QT (Shimadzu Corporation, Kyoto, Japan) (Figure 1B). Mass spectrum were obtained in the *m/z* 300-330 range in both positive and negative ion modes. Product ion spectrum were obtained in the m/z range of 100-330 in the positive ion detection mode. The laser intensity was set to 65 and the laser irradiation diameter was set to 2 (both in arbitrary units). These analysis conditions are summarized in Table 1. After analysis, image reconstruction and peak intensity extraction were performed using the data analysis software IMAGEREVEAL™ MS (Shimadzu Corporation, Kyoto, Japan) (Figure 1C).

(A)

(C)

(B)

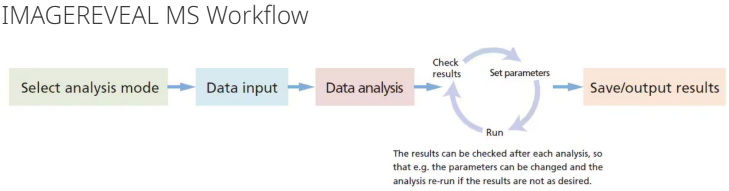

Figure 1 (A) Matrix deposition system iMLayer™ , (B) Imaging mass microscope iMScope™ QT, (C) Data analysis software IMAGEREVEAL™ MS

Table 1 MSI Analysis Parameters

MS Analysis Conditions	
Ion mode	Positive
m/z range	300-330（MS）、100-330（MS/MS）
Accumulation number of times	1
DL temperature	250 °C
Heat block temperature	450 °C
Sample Voltage	4.50 kV
Detector voltage *	2.10 kV（Standard）、2.30 kV（Sections）
MS steps	1 or 2
CID gas pressure	150 kPa（MS1）、230 kPa（MS/MS）
Laser irradiation conditions	
Number of shots	80 shots
Repetition frequency	1000 Hz
irradiation diameter set value	2
Laser Power	65

*：Reference value
The optimum detector voltage depends on the degree of detector degradation and the ease of ionization of the sample. Some detector voltage settings may accelerate detector deterioration. Please refer to the instruction manual for details.

3. Results

3-1. Confirmation of Ionization Using Ethaboxam Standard.
Figure 2 shows the chemical structure formula of ethaboxam and the mass spectrum and product ion spectrum obtained in positive ion mode using α-CHCA. As shown in Figure 2(A), the $[M+H]^+$ is expected to be detected with positive ion mode at *m/z* 321.08, and this ion was detected in the mass spectrum of the ethaboxam standard with α-CHCA matrix in Figure 2(B left). On the other hand, no peak was detected in the negative ion mode with 9-AA (data not shown).

In addition, we checked whether product ions were detected from *m/z* 321.08, which was detected with positive ion mode. As a result, product ions were detected at *m/z* 183.05, 200.07, and 237.08 as shown in Figure 2 (B right). The dissociated portions of each product ion are shown in Figure 2(A). From the above, we decided to use the positive ion mode with α-CHCA in the subsequent experiments. The peak at *m/z* 321.08 or *m/z* 183.05, which was the base peak in the product ion spectrum, was used to generate imaging results.

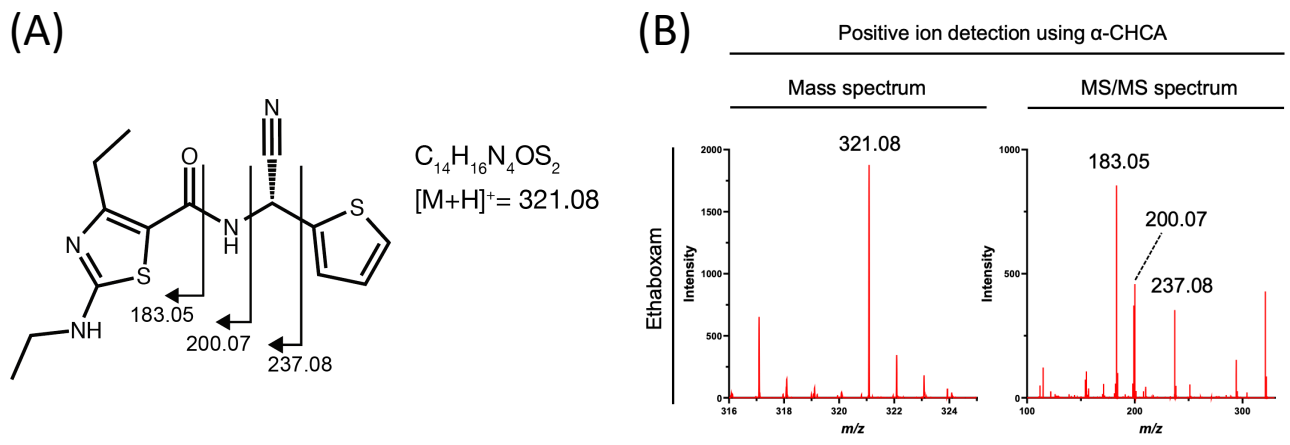

Figure 2. Chemical structural formula of ethaboxam and MS and MS/MS spectrum of ethaboxam standard.
(A) The chemical structural formula of ethaboxam and expected *m/z* upon detection.
(B) Mass spectrum and product ion spectrum of ethaboxam standard obtained by iMScope QT.

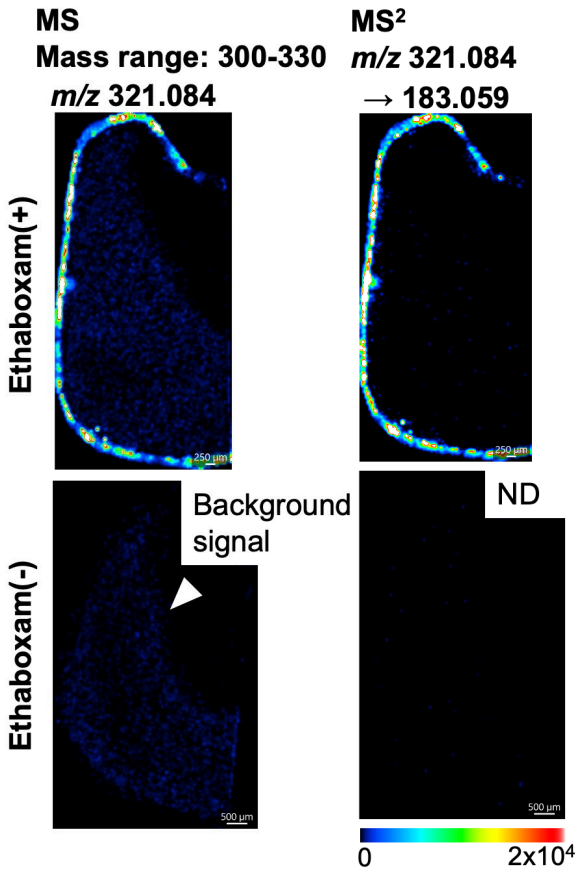

Figure 3 MS Imaging of corn seed sections obtained with and without ethaboxam treatment.
Scale bar: 250 µm (ethaboxam treated), 500 µm (ethaboxam untreated)

3-2. comparison of MS imaging results by mass spectrum and product ion spectrum.
Figure 3 shows the MS imaging results of corn seeds by mass spectrum and by product ion spectrum. In both cases, we can see that ethaboxam accumulates on the seed surface. In the negative control Ethaboxam (-), which was treated with ultrapure water instead of ethaboxam, the MS imaging results using mass spectrum show a faint signal distribution (arrowheads). This was found to be background noise due to foreign peaks near the ethaboxam-derived peak. On the other hand, the imaging results using the product ion spectrum showed that no background noise of biological origin was detected in the negative control, and an image of the distribution of immersed ethaboxam was obtained. Based on these results, we decided to perform MALDI-MSI using the product ion spectrum in our future experiments.

3-3. MALDI-MSI in Seeds before Sowing.
Figure 4 shows the results of ethaboxam imaging in seeds before sowing in soil. Figure 4(A) represents soybean and Figure 4(B) represents corn. In the negative control, no distribution of ethaboxam-derived peaks is obtained, while in the ethaboxam-coated seeds, ethaboxam-derived peaks can be seen mainly on the seed surface in both seeds. Furthermore, in corn, accumulation of ethaboxam not only on the seed surface but also at the germ tip and penetration into the endosperm were observed (arrowheads in Figure 4B). These results suggest that the distribution of ethaboxam is different between soybean and corn seeds, even with similar coating treatments, and therefore the pesticide dynamics after seeding is also expected to be different.

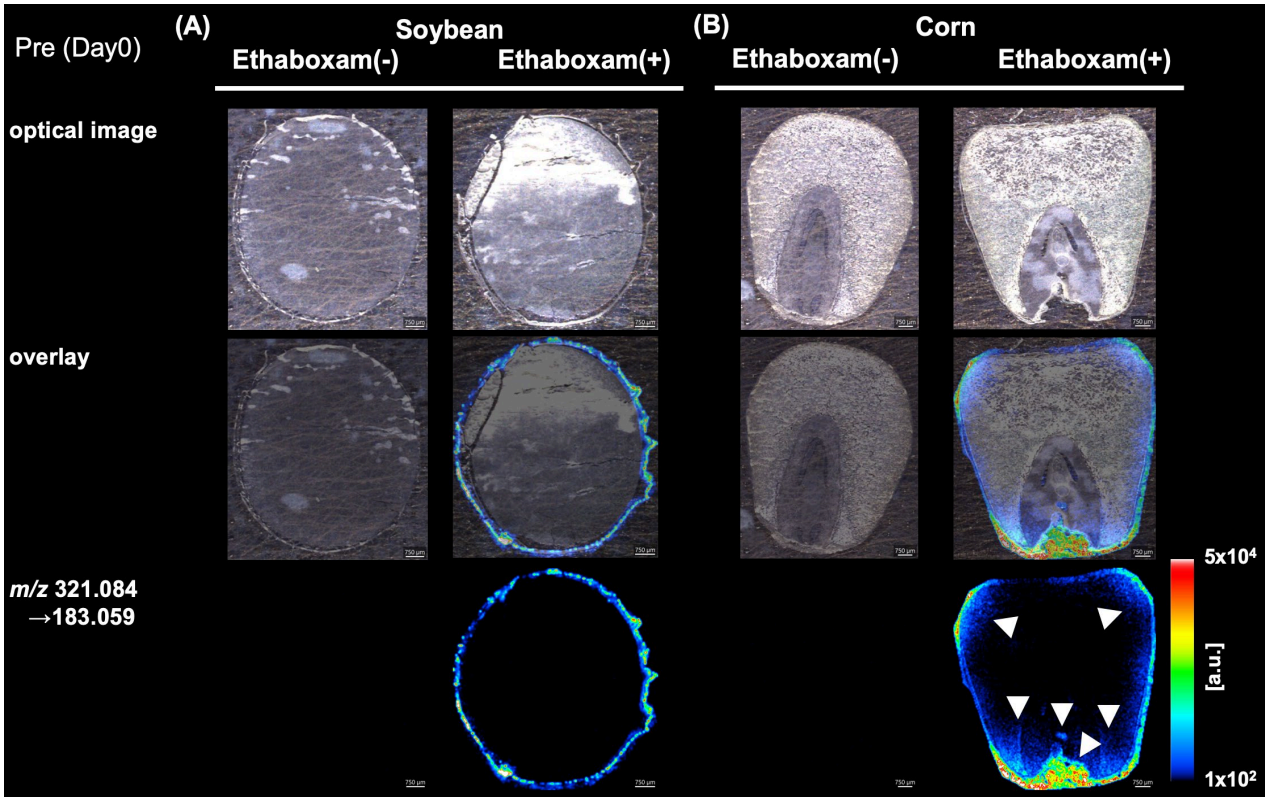

Figure 4. distribution of ethaboxam in soybean and corn seeds before sowing in soil.
(A) Soybean seed (B) Corn seed
Upper: optical image, center: superimposed optical image and MS image, lower: ethaboxam distribution. Scale bar: 750 µm

3-4. MALDI-MSI in Seeds after Sowing.
Figure 5 shows the distribution of ethaboxam in seed sections at 5 days after sowing in soil. Figure 5(A) shows soybean seeds and Figure 5(B) shows corn seeds. In soybean seeds, the ion intensity is very weak compared to that before seeding as shown in Figure 4, suggesting that the ethaboxam accumulated in the soybean epidermis may have migrated mainly to the soil. On the other hand, in the corn seed shown in Figure 5(B), accumulation in the epidermis was still observed on the 5th day, and at the same time, the ion intensity derived from ethaboxam increased in the embryo part (arrowhead in Figure 5B). This suggests that the ethaboxam accumulated at the germ tip migrates into the soil and also into the interior of the seed. From the above, soybean and corn, which showed different distributions at the seed point before sowing, are expected to show different pesticide dynamics after sowing.

3-5. comparison of ion intensities obtained from MALDI-MSI results.
Figure 6 and Figure 7 show a comparison of ion intensities obtained from MALDI-MSI results. Figure 6 shows soybean seeds and Figure 7 shows corn seeds. In this graph, intensity extraction was performed separately for the epidermis and interior at pre-sowing, 1 and 5 days after sowing (Verification was conducted with three grains each of soybeans and corn). Figure 6 shows that the ion intensity in the epidermis of soybean seeds decreased rapidly from day 1 to day 5 after sowing. The increase in ion intensity inside the seed was negligible. This suggests that in soybean, ethaboxam does not migrate into the interior of the seed, and that the main route is into the soil. On the other hand, in corn, shown in Figure 7, the accumulation in the epidermis is maintained after sowing, while at the same time the internal translocation increases significantly at 5 days. This indicates that, unlike soybean seeds, corn seeds not only migrate into the soil, but also into the interior of the seed. These results indicate that pesticide dynamics are different between soybean seeds and corn seeds, even in the same seed coat.

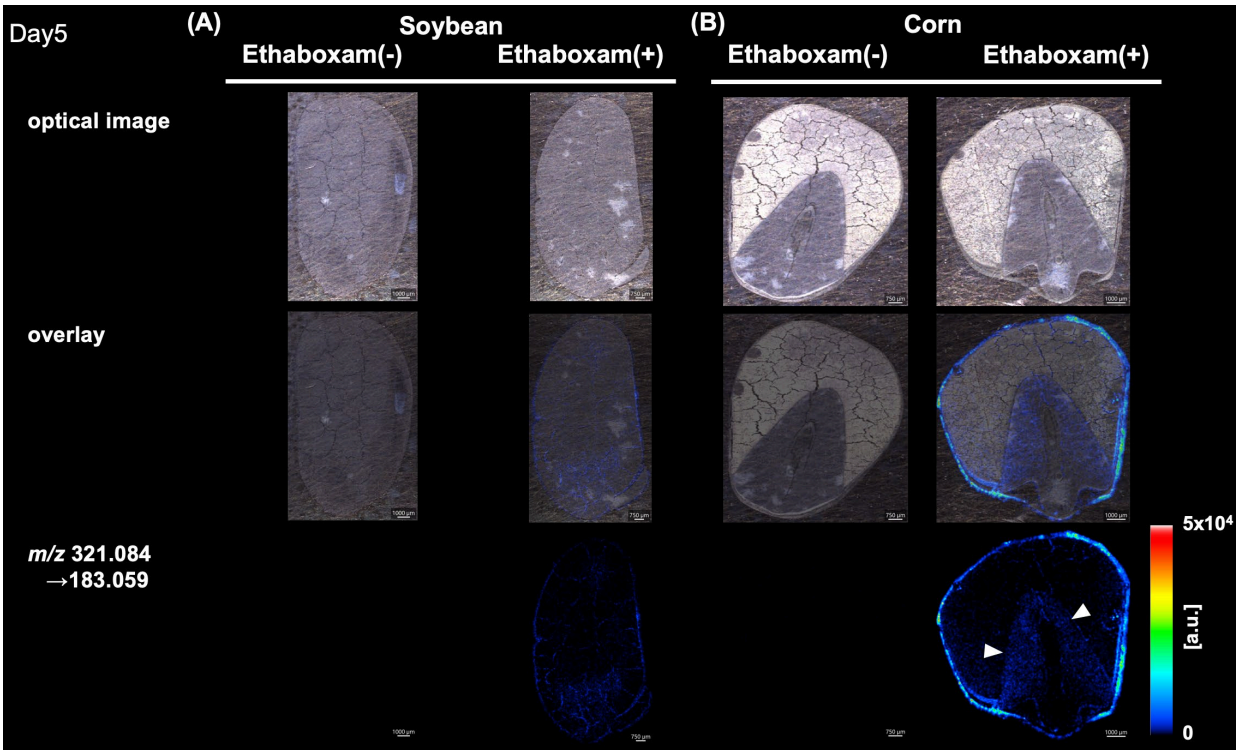

Figure 5. ethaboxam distribution in soybean and corn seeds 5 days after sowing in soil.
(A) Soybean seed (B) Corn seed
In soybean seeds, ethaboxam-derived ions are observed, but their intensity is weak. On the other hand, in corn seeds, ethaboxam accumulates in the embryo part as well as in the epidermis.

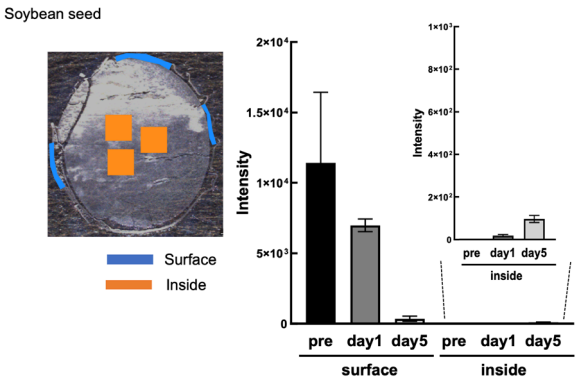

Figure 6: Comparison of ion intensity in soybean seeds.
Accumulation is found mainly on the epidermis, with a marked decrease in intensity by day 5, suggesting little accumulation on the seed surface or transfer to the interior.

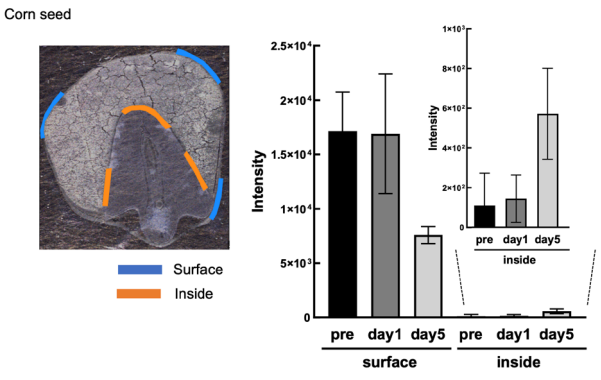

Figure 7: Comparison of ion intensity in corn seeds.
Accumulation in the epidermis as well as migration into the seed interior was observed (migration into the seed interior on day 5 was about 1/10 of that into the epidermis).

4. Discussion

When corn seeds treated with ethaboxam for pesticide seed treatment germinated, ethaboxam-derived ions were also detected inside the seeds, and ethaboxam accumulation was also observed in the hypocotyl and pericarp. In contrast, in soybean seeds, the ion intensity was strongest on the seed coat and decreased from the seed coat surface toward the seed interior. The ion intensity also decreased dramatically at day 5. These results suggest that in soybean seeds coated with ethaboxam, the pesticide mainly stays on the seed coat surface and is released into the soil over time. The differences in the distribution of ethaboxam observed after sowing are presumably related to differences in seed structure, particularly the presence or absence of endosperm. In corn seeds, which are endosperm seeds, ethaboxam accumulation was detected in the embryo after the seeds were coated with the pesticide. Therefore, if the distribution of the pesticide differed significantly at the pre-sowing stage, it was expected that the movement of the pesticide would also have a significant impact on this difference. In fact, the intensity graphs of ethaboxam on the surface and embryo of corn seeds after sowing showed a significant shift in distribution pattern from day 1 to day 5 compared to soybean seeds, with a marked shift from the embryo to the endosperm. In other words, it can be concluded that the treated seeds began to move the ethaboxam into the seed interior.. In the case of soybean seeds, on the other hand, ethaboxam was detected on the seed surface on the first day after sowing, but the amount detected inside the seed was smaller. This trend became more pronounced on the fifth day after sowing, which may indicate that ethaboxam rarely migrates directly from the seed coat to the seed interior..

5. Summary

Seed treatments are transferred to plant tissues by direct transfer to the plant or indirect transfer through the soil to protect against plant pathogens. By visualizing the localization of the active compounds along with the seed substructure, we were able to obtain data suggesting that the migration ratios of the compounds varied with seed type and structure. Such behavior of seed-treated compounds may depend on the physical properties of each chemical and the species-specific seed structure. Therefore, in the future, MALDI-MSI using iMScope QT is expected to help in the development of seed treatment methods, such as formulation optimization, by understanding the distribution of chemical compounds in the target seeds.

<Reference>

1) Shimma, S., Saito, H., Inoue, T., and Iwahashi, F., Using mass spectrometry imaging to visualize pesticide accumulation and time-dependent distribution in fungicide-coated seeds, Mass Spectrom (available online).
2) Shimma, S., Kumada, H. O., Taniguchi, H., Konno, A., Yao, I., Furuta, K., Matsuda, T., and Ito, S.: Microscopic visualization of testosterone in mouse testis by use of imaging mass spectrometry, Anal Bioanal Chem, 408, 7607-7615 (2016).
3) Sugiura, Y., Takeo, E., Shimma, S., Yokota, M., Higashi, T., Seki, T., Mizuno, Y., Oya, M., Kosaka, T., Omura, M., and other authors: Aldosterone and 18-Oxocortisol Coaccumulation in Aldosterone-Producing Lesions, Hypertension, 72, 1345-1354 (2018).
4) Dalisay, D. S., Kim, K. W., Lee, C., Yang, H., Rubel, O., Bowen, B. P., Davin, L. B., and Lewis, N. G.: Dirigent Protein-Mediated Lignan and Cyanogenic Glucoside Formation in Flax Seed: Integrated Omics and MALDI Mass Spectrometry Imaging, J. Nat. Prod., 78, 1231-1242 (2015).
5) Crecelius, A. C., Holscher, D., Hoffmann, T., Schneider, B., Fischer, T. C., Hanke, M. V., Flachowsky, H., Schwab, W., and Schubert, U. S.: Spatial and Temporal Localization of Flavonoid Metabolites in Strawberry Fruit (Fragaria x ananassa), J Agric Food Chem, 65, 3559-3568 (2017).
6) Nguyen, T. B., Kitani, S., Shimma, S., and Nihira, T.: Butenolides from Streptomyces albus J1074 Act as External Signals To Stimulate Avermectin Production in Streptomyces avermitilis, Appl Environ Microbiol, 84 (2018).
7) Miyoshi, K., Enomoto, Y., Fukusaki, E., and Shimma, S.: Visualization of Asparaptine in Asparagus (Asparagus officinalis) Using MALDI-IMS, Anal. Sci., 34, 997-1001 (2018).
8) Dunham, S. J. B., Ellis, J. F., Li, B., and Sweedler, J. V.: Mass Spectrometry Imaging of Complex Microbial Communities, Acc. Chem. Res., 50, 96-104 (2017).
9) Ikuta S, Fukusaki E, Shimma S. Visualization of azoxystrobin penetration in wheat leaves using mass microscopy imaging. J. Pestic. Sci., 48, 29–34 (2023).
10) Mullen, A. K., Clench, M. R., Crosland, S., and Sharples, K. R.: Determination of agrochemical compounds in soya plants by imaging matrix-assisted laser desorption/ionisation mass spectrometry, Rapid Commun. Mass Spectrom., 19, 2507-2516 (2005).
11) Fadel Sartori, F., Floriano Pimpinato, R., Tornisielo, V. L., Dieminger Engroff, T., de Souza Jaccoud-Filho, D., Menten, J. O., Dorrance, A. E., and Dourado-Neto, D.: Soybean seed treatment: how do fungicides translocate in plants?, Pest Manag Sci, 76, 2355-2359 (2020).
12) Sharma, K. K., Singh, U. S., Sharma, P., Kumar, A., and Sharma, L.: Seed treatments for sustainable agriculture-A review, Journal of Applied and Natural Science, 7, 521-539 (2015).
13) Dorrance, A. E. and McClure, S. A.: Beneficial Effects of Fungicide Seed Treatments for Soybean Cultivars with Partial Resistance to Phytophthora sojae, Plant Dis., 85, 1063-1068 (2001).
14) Ellis, M. L., Broders, K. D., Paul, P. A., and Dorrance, A. E.: Infection of Soybean Seed by Fusarium graminearum and Effect of Seed Treatments on Disease Under Controlled Conditions, Plant Dis., 95, 401-407 (2011).
15) Alford, A. and Krupke, C.H.: Translocation of the neonicotinoid seed treatment clothianidin in maize, PLOS ONE, 12, e0186527 (2017).
16) Kim, D. S., Chun, S. J., Jeon, J. J., Lee, S. W., and Joe, G. H.: Synthesis and fungicidal activity of ethaboxam against Oomycetes, Pest Manag Sci, 60, 1007-1012 (2004).
17) Hao, W., Gray, M. A., Förster, H., and Adaskaveg, J. E.: Evaluation of New Oomycota Fungicides for Management of Phytophthora Root Rot of Citrus in California, Plant Dis., 103, 619-628 (2019).
18) Scott, K., Eyre, M., McDuffee, D., and Dorrance, A. E.: The Efficacy of Ethaboxam as a Soybean Seed Treatment Toward Phytophthora, Phytopythium, and Pythium in Ohio, Plant Dis., 104, 1421-1432 (2020).

First Edition: Sep. 2024

SHIMADZU
Shimadzu Corporation
www.shimadzu.com/an/

› Please fill out the survey

Related Products Some products may be updated to newer models.

› iMScope QT
Imaging Mass Microscope

› IMAGEREVEAL MS
Mass Spectrometry Imaging Data Analysis Software

› iMLayer
Matrix Vapor Deposition System

Related Solutions

› Life Science

› Food and Beverages

› Residual Pesticides

› Price Inquiry

› Product Inquiry

› Technical Service / Support Inquiry

› Other Inquiry